

# Performance Assessment and Design for Univariate Alarm Systems Based on FAR, MAR, and AAD

Jianwei Xu, Jiandong Wang, Iman Izadi, and Tongwen Chen, *Fellow, IEEE*

**Abstract**—The performance of a univariate alarm system can be assessed in many cases by three indices, namely, the false alarm rate (FAR), missed alarm rate (MAR), and averaged alarm delay (AAD). First, this paper studies the definition and computation of the FAR, MAR, and AAD for the basic mechanism of alarm generation solely based on a trip point, and for the advanced mechanism of alarm generation by exploiting alarm on/off delays. Second, a systematic design of alarm systems is investigated based on the three performance indices and the tradeoffs among them. The computation of FAR, MAR, and AAD and the design of alarm systems require the probability density functions (PDFs) of the univariate process variable in the normal and abnormal conditions. Thus, a new method based on mean change detection is proposed to estimate the two PDFs. Numerical examples and an industrial case study are provided to validate the obtained theoretical results on the FAR, MAR and AAD, and to illustrate the proposed performance assessment and alarm system design procedures.

**Note to Practitioners**—Alarm systems are critically important to the safety and efficient operation of modern industrial plants, whose operations are monitored by continuous measurements of various signals. However, industrial surveys have shown that operators of industrial plants receive far more alarms, many of which belong to nuisance alarms, than they can handle. Relieving this problem is based upon a satisfactory performance of the alarm system for each univariate signal involved in the operation of industrial plants. This paper studies the performance assessment and design of univariate alarm systems for basic mechanism of alarm generation and for advanced one exploiting alarm on/off delays. The obtained results are applicable to various industrial plants including power, chemical, and petrochemical plants.

**Index Terms**—Averaged alarm delay (AAD), change detection, false alarm rate (FAR), kernel PDFs, missed alarm rate (MAR), performance assessment, univariate alarm systems.

## I. INTRODUCTION

LARM systems are critically important to the safety and efficient operation of modern industrial plants. The performance of alarm systems has received increasing attention

Manuscript received September 19, 2011; accepted October 29, 2011. Date of publication December 08, 2011; date of current version April 03, 2012. This paper was recommended for publication by Associate Editor Q. Ha and Editor M. Zhou upon evaluation of the reviewers' comments. This work was supported in part by the Shandong Electric Power Research Institute, NSERC, and the National Natural Science Foundation of China under Grant 60704031, Grant 61061130559, and Grant 10832006.

J. Xu and J. Wang are with the College of Engineering, Peking University, Beijing, China 100871 (e-mail: xujianwei919@pku.edu.cn; jiandong@pku.edu.cn).

I. Izadi is with Matrikon Inc., Edmonton, AB T5J 3N4, Canada (e-mail: iman.izadi@matrikon.com).

T. Chen is with the Department of Electrical and Computer Engineering, University of Alberta, Edmonton, AB T6G 2V4, Canada (e-mail: tchen@ece.ualberta.ca).

Digital Object Identifier 10.1109/TASE.2011.2176490

from both industrial and academic communities [1], [2], [4], [5], [9]–[14], [17], [19], [21]–[24].

The performance of alarm systems can be measured via basic activation metrics such as the number of alarms per hour, peak number of alarms per hour, number of high/low priority alarms per hour, and alarm acknowledge ratio [4], [17]. For a univariate alarm system, its performance can be assessed in many cases by three indices, namely, the false alarm rate (FAR), missed alarm rate (MAR), and averaged alarm delay (AAD). The FAR and MAR measure the accuracy of an alarm system in detecting the normal and abnormal conditions for the process variable being monitored. A high value of FAR implies a large amount of false alarms that would unnecessarily disturb operators. If the MAR is excessive, then the designed functionality of alarm systems would be severely degraded. The AAD measures the alarm latency or promptness of the alarm system. If the AAD is smaller, then the alarm becomes active more promptly after the process variable being monitored runs into the abnormal condition, which leaves operators more time to respond to the alarm.

If the performance of alarm systems is not satisfactory, then a new design of alarm systems is often required. The alarm limits are suggested to change in a time-varying manner according to recent mean and standard deviation values [8], [14], [19]. The alarm settings are determined based on the probability that an alarm will occur for values preceding the alarm trip point, and the probability that the process will continue on to a value following activating alarms [10]. A geometric process control method is proposed to deliver dynamically varying alarm limits for multivariate alarm signals [5]. The guideline for setting the deadband values is proposed in [11] to handle chattering alarms. The alarm limits for correlated signals are selected to preserve their correlation relationship for alarm data [23]. The design of optimal linear and nonlinear filters for alarm systems are studied in [7]. To the best of our knowledge, however, a systematic design procedure for univariate alarm systems to satisfy the performance indices including FAR, MAR, and AAD may not be available in the literature, except our earlier works in [12] and [21].

In this paper, we will first investigate the definition and computation of the FAR, MAR and AAD for the basic mechanism of alarm generation solely based on a trip point, and for the advanced mechanism of alarm generation by exploiting alarm on/off delays. Second, we will propose a systematic design procedure to choose the trip point and/or the number of sample delay for alarm systems based on the FAR, MAR and AAD, and the tradeoffs among them. The computation of FAR, MAR and AAD and the design of alarm systems require the probability density functions (PDFs) of the univariate process variable in the normal and abnormal conditions. Thus, the third contribu-

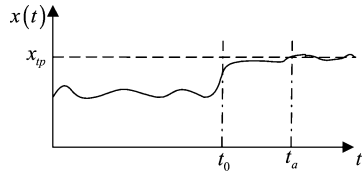


Fig. 1. The measurement  $x(t)$  of the process variable  $x$  with a variation from normal condition to abnormal one at the time instant  $t_0$ .

tion of this paper is to propose a new method to estimate the two PDFs under some mild assumptions. The new method exploits mean change detection techniques and statistical hypothesis tests for separation of the normal and abnormal data, from which the kernel-based method is used to estimate the PDFs. Several numerical examples and an industrial case study are provided to validate the obtained theoretical results on the FAR, MAR and AAD and to illustrate the proposed performance assessment and alarm system design procedures. This paper is a continuing study of our earlier works in [12] and [21], which presented some preliminary results for the above first two contributions.

The rest of this paper is organized as follows. Section II is devoted to the definition and computation of the FAR, MAR and AAD for the basic mechanism of alarm generation. Section III studies the FAR, MAR, and AAD for alarm on/off delay. A systematic design procedure for alarm systems is investigated in Section IV. Section V proposes the new method for estimating the PDFs of the process variable being monitored in the normal and abnormal conditions. Section VI provides an industrial case study to illustrate the performance assessment and alarm system design procedures in practice. Finally, some concluding remarks are given in Section VII.

## II. PERFORMANCE INDICES FOR BASIC ALARM GENERATION MECHANISM

This section studies the three performance indices, namely, the FAR, MAR and AAD, for the basic alarm generation mechanism used in industry.

Consider the measurement of a process variable  $x$ , denoted as a discrete-time signal  $x(t)$  with sampling period  $h$  and its associated alarm trip point  $x_{tp}$  depicted in Fig. 1. For the basic alarm generation mechanism, an alarm is raised if  $x(t)$  exceeds  $x_{tp}$ . Due to various reasons, including the randomness of  $x(t)$  and improper selection of  $x_{tp}$ , two types of undesired alarms may appear, namely, the false and missed alarms. A false alarm is an alarm that is raised when the process variable  $x$  is behaving normally; missed alarms occur when the process variable  $x$  is behaving abnormally but no alarm is raised. The false alarms may lead to losing the trusty of alarm systems due to “cry wolf” effect, while the missed alarms would severely degrade the designed functionality of alarm systems. Hence, the FAR and MAR are the two important indices to assess the performance of alarm systems.

For the time being, let us assume that the PDFs of the process variable  $x$  in the normal and abnormal conditions are known *a priori*; the PDFs will be estimated from the measurements of  $x$  later in Section V. Fig. 2 illustrates the PDFs, together with the

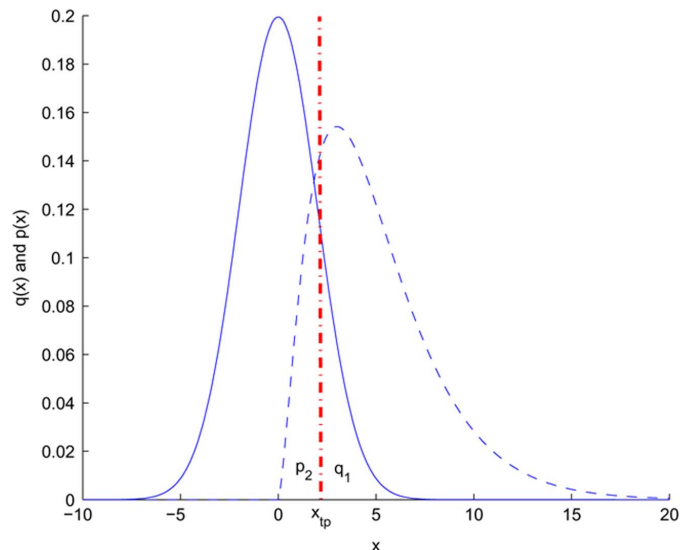


Fig. 2. The PDFs of  $x$  under normal and abnormal conditions.

trip point  $x_{tp}$ . Denote the PDF for the normal condition as  $q(x)$  (solid line in Fig. 2). The FAR as the probability of false alarms is the area under the distribution curve  $q(x)$  for the values of  $x$  greater than the trip point  $x_{tp}$ , i.e.,

$$\text{FAR} = \int_{x_{tp}}^{+\infty} q(x)dx. \quad (1)$$

In Fig. 2, the FAR is denoted by  $q_1$ . Similarly, the MAR, the probability of missed alarms is

$$\text{MAR} = \int_{-\infty}^{x_{tp}} p(x)dx \quad (2)$$

where  $p(x)$  is the PDF of  $x$  in the abnormal condition (dashed line in Fig. 2). In Fig. 2, the MAR is denoted by  $p_2$ .

Besides the FAR and MAR, the AAD is another important performance index for alarm systems. Suppose that the process variable  $x$  in Fig. 1 is experiencing a variation from normal condition to abnormal one at the time instant  $t_0$ . Denote  $t_a$  as the time instant when the first sample point of  $x(t)$  is equal to or larger than the trip point  $x_{tp}$  so that the alarm is raised. The time difference between  $t_0$  and  $t_a$  is named as the alarm delay, i.e.,

$$T_d = t_a - t_0.$$

Because of sampling,  $T_d$  is a discrete random variable with the sample space  $\{0h, 1h, 2h, \dots\}$ , where  $h$  is the sample period. Note that  $t_a \geq t_0$  so that  $T_d$  is always nonnegative since false alarms ahead of  $t_0$  should not be considered in order to have a physically meaningful interpretation of the alarm delay. The AAD is defined as the expected value of  $T_d$

$$\bar{T}_d = E(T_d). \quad (3)$$

The AAD measures the promptness of the alarm system: if  $\bar{T}_d$  is smaller, then the alarm is raised more promptly after  $x(t)$  runs into the abnormal condition, which leaves operators more time to respond to the alarm.

In general, the computation of  $\bar{T}_d$  requires the knowledge of multidimensional joint PDFs of  $x(t_0), x(t_0 + h), \dots$ . For simplicity,  $x(t)$  is assumed here to be independent and identically distributed (IID). For  $t \geq t_0$  (i.e.,  $x$  is under the abnormal condition), the PDF of  $x$  is  $p(x)$  (the dashed line in Fig. 2), and as defined earlier in (2),  $p_2$  is the probability of  $x$  with the PDF  $p(x)$  less than the trip point  $x_{tp}$ . For ease of notations,  $p_1 := 1 - p_2$ . As  $x(t)$  is IID, the probability mass function of  $T_d = ih$  is

$$P(T_d = ih) = P(x(t_0) < x_{tp}, \dots, x(t_0 + ih - h) < x_{tp}, \\ x(t_0 + ih) > x_{tp}) = p_2^i p_1.$$

Thus, the time delay  $T_d$  follows a geometric distribution; using the mean expression of a geometric random variable (e.g., [20, pp. 134–135]), the AAD is

$$\bar{T}_d = E(T_d) = \sum_{i=0}^{\infty} i h p_2^i p_1 = h \frac{p_2}{p_1}. \quad (4)$$

*Example 1:* This example is to validate the FAR in (1), MAR in (2), and AAD in (4) via simulation. The process variable  $x$  is generated as a white Gaussian random process with a mean change at  $t_0$ , i.e.,

$$\begin{cases} x(t) \sim N(3, 1), & t < t_0 \\ x(t) \sim N(5, 1), & t \geq t_0 \end{cases}. \quad (5)$$

The change time is  $t_0 = 1000h$  with the sampling period  $h = 1$  s. The length of the data is 2000. The trip point  $x_{tp} = 4$ . Equations (1), (2), and (4) yield the theoretical values of the FAR, MAR, and AAD

$$\text{FAR} = 0.1587, \text{ MAR} = 0.1587, \bar{T}_d = 0.1886.$$

To verify these theoretical values, 500 independent realizations of the sequence  $\{x(t)\}_{t=1}^{2000}$  are generated; for each realization, a single estimate FAR (MAR) is provided as the ratio between the observed number of alarms (no-alarms) to the data length of  $x(t)$  in the normal (abnormal) condition (equal to 1000 here). Based on the 500 independent realizations, the sample mean and standard deviation of FAR (MAR) can be obtained

$$\begin{aligned} m(\hat{\text{FAR}}) &= 0.1589, & s(\hat{\text{FAR}}) &= 0.0115 \\ m(\hat{\text{MAR}}) &= 0.1589, & s(\hat{\text{MAR}}) &= 0.0118 \end{aligned}$$

which are consistent with the theoretical values.

Since the actual change time  $t_0$  is available, the alarm delay for each realization is observed. The average of the alarm delays in the 500 independent realizations is regarded as one sample of the AAD, denoted as  $\hat{T}_d$ . To obtain a number of such samples, 600 sets of the above 500 independent realizations are generated, which provide 600 samples of  $\hat{T}_d$ . The sample mean and standard deviation of these 600 samples are

$$m(\hat{T}_d) = 0.1875, \quad s(\hat{T}_d) = 0.0206$$

which support the theoretical value  $\bar{T}_d = 0.1886$ .  $\square$

### III. PERFORMANCE INDICES FOR ALARM ON/OFF DELAY

This section studies the FAR, MAR, and AAD for the alarm on/off delay [2], also known as alarm delay timer [4], which is

widely used in practice. With the alarm on/off delay, an alarm will be raised/cleared if and only if more than  $n$  consecutive samples of  $x(t)$  in Fig. 1 are larger/smaller than the trip point  $x_{tp}$ . Thus, the basic alarm generation mechanism in Section II can be regarded as a special case for the number of sample delay  $n = 1$ . This section develops the corresponding FAR, MAR and AAD when the on/off-delay is exploited.

The  $n$ -sample alarm on/off delay involves  $n$  no-alarm states and  $n$  alarm states, and its working mechanism can be described by Markov chains. The transition among these states for the process variable  $x$  in the normal condition is represented by the Markov chain in Fig. 3. For  $x$  in the normal condition, the PDF of  $x$  is  $q(x)$  (the solid line in Fig. 2); as defined earlier in (1),  $q_1$  is the probability of  $x$  with the PDF  $q(x)$  greater than the trip point  $x_{tp}$ , and for ease of notations,  $q_2 := 1 - q_1$ . If the alarm on/off delay for a certain sample  $x(t_1)$  is at the  $i$ th no-alarm state  $NA_i$  for  $i = 1, 2, \dots, n$ , and the next sample  $x(t_1 + h)$  ( $h$  is the sampling period) exceeds  $x_{tp}$ , then the current state  $NA_i$  goes to the  $(i+1)$ th no-alarm state  $NA_{i+1}$  for  $i < n$ , or to the alarm state  $A_1$  for  $i = n$ . If  $x(t_1 + h)$  is less than  $x_{tp}$ , then the current state  $NA_i$  directly goes back to the first no-alarm state  $NA_1$ . Similarly, if the alarm on/off delay for a certain sample  $x(t_2)$  is at the  $i$ th alarm state  $A_i$  for  $i = 1, 2, \dots, n$ , and the next sample  $x(t_2 + h)$  is less than  $x_{tp}$ , then the state  $A_i$  goes to the  $(i+1)$ th alarm state  $A_{i+1}$  for  $i < n$ , or to the no-alarm state  $NA_1$  for  $i = n$ . If  $x(t_2 + h)$  is larger than  $x_{tp}$ , then the state  $A_i$  goes back to the first alarm state  $A_1$ .

*Proposition 1:* For the  $n$ -sample alarm on/off delay, the FAR is

$$\text{FAR} = \frac{q_1^n (1 + q_2 + \dots + q_2^{n-1})}{q_1^n (1 + q_2 + \dots + q_2^{n-1}) + q_2^n (1 + q_1 + \dots + q_1^{n-1})} \quad (6)$$

*Proof of Proposition 1:* To simplify the notation, the states  $NA_1, NA_2, \dots, NA_n, A_1, \dots, A_n$  are defined as the states  $1, 2, \dots, n-1, n, \dots, 2n$ , respectively. Let  $T_{i,k}$  be the number of steps taken for the transmission from state  $i$  to another state  $k$ , and  $P_{i,k}^{(l)}$  as the probability of  $T_{i,k} = l$ , i.e.,

$$P_{i,k}^{(l)} := P(T_{i,k} = l).$$

When  $l = 1$ ,  $P_{i,k}^{(1)}$  denotes the one step transition probability. For the Markov chain in Fig. 3, the matrix  $Q \in \mathbb{R}^{2n \times 2n}$  of one step transition probability is

$$Q = \begin{bmatrix} q_2 & q_1 & 0 & \cdots & 0 & 0 & 0 & \cdots & 0 \\ q_2 & 0 & q_1 & \cdots & 0 & 0 & 0 & \cdots & 0 \\ \vdots & \vdots & \vdots & \ddots & \vdots & \vdots & \vdots & \ddots & \vdots \\ q_2 & 0 & \cdots & 0 & q_1 & 0 & 0 & \cdots & 0 \\ 0 & 0 & \cdots & 0 & q_1 & q_2 & 0 & \cdots & 0 \\ 0 & 0 & 0 & \cdots & q_1 & 0 & q_2 & \cdots & 0 \\ \vdots & \ddots & \vdots \\ 0 & 0 & 0 & \cdots & q_1 & 0 & 0 & \cdots & q_2 \\ q_2 & 0 & 0 & \cdots & q_1 & 0 & 0 & \cdots & 0 \end{bmatrix}.$$

Here, the element locating at  $i$ th row and the  $j$ th column of the matrix  $Q$  is the one step transition probability of the state from  $i$  to  $j$ . Based on the theory of the stationary distribution

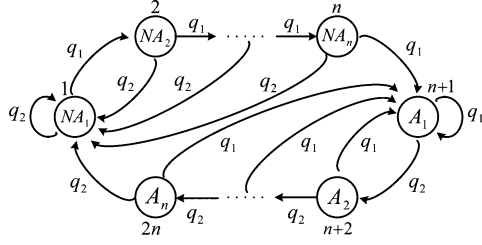


Fig. 3. Markov chain for the  $n$ -sample alarm on/off delay of  $x(t)$  in the normal condition.

[15, pp. 727–729], for an irreducible ergodic Markov chain, the limiting probabilities

$$\pi_k = \lim_{l \rightarrow \infty} P_{ik}^{(l)} > 0$$

exist, being independent of the initial state, and satisfy the equality

$$\sum_k \pi_k = 1. \quad (7)$$

Because the Markov chain has only a finite number of states, these limiting probabilities satisfy the equality

$$\Pi = \Pi Q \quad (8)$$

where

$$\Pi = [\pi_1 \ \pi_2 \ \dots \ \pi_{2n}].$$

Rewrite (8) as

$$\begin{cases} q_2(\pi_1 + \dots + \pi_n) + q_2\pi_{2n} = \pi_1 \\ q_1\pi_1 = \pi_2 \\ q_1\pi_2 = \pi_3 \\ \vdots \\ q_1\pi_{n-1} = \pi_n \\ q_1(\pi_n + \dots + \pi_{2n}) = \pi_{n+1} \\ q_2\pi_{n+1} = \pi_{n+2} \\ \vdots \\ q_2\pi_{2n-1} = \pi_{2n} \end{cases}. \quad (9)$$

From (9), we have

$$\begin{cases} \pi_2 = q_1\pi_1 \\ \vdots \\ \pi_n = q_1^{n-1}\pi_1 \end{cases} \quad (10)$$

and

$$\begin{cases} \pi_{n+2} = q_2\pi_{n+1} \\ \vdots \\ \pi_{2n} = q_2^{n-1}\pi_{n+1} \end{cases}. \quad (11)$$

Using (10) and (11), (7) and the first equality in (9) can be, respectively, written as

$$\begin{cases} \pi_1(1+q_1+\dots+q_1^{n-1}) + \pi_{n+1}(1+q_2+\dots+q_2^{n-1}) = 1 \\ q_2\pi_1(1+q_1+\dots+q_1^{n-1}) + q_2^n\pi_{n+1} = \pi_1 \end{cases}$$

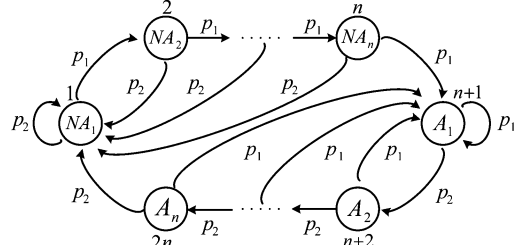


Fig. 4. Markov diagram with  $n$ -sample delay of  $x(t)$  in the abnormal condition.

from which  $\pi_{n+1}$  is obtained as

$$\pi_{n+1} = \frac{q_1^n}{q_1^n(1+q_2+\dots+q_2^{n-1}) + q_2^n(1+q_1+\dots+q_1^{n-1})}. \quad (12)$$

From the Markov chain in Fig. 3, the FAR is the sum of probabilities of all the alarm states

$$\begin{aligned} \text{FAR} &= P(A_1) + P(A_2) + \dots + P(A_n) \\ &= \pi_{n+1} + \dots + \pi_{2n} \\ &= \pi_{n+1}(1+q_2+\dots+q_2^{n-1}) \end{aligned}$$

where the last equality is from (11). This result, together with (12), proves (6).  $\square$

The state transition for  $x(t)$  in the abnormal condition is presented by the Markov chain in Fig. 4, where  $p_2$  is the probability of  $x$  with the PDF  $p(x)$  (the dashed line in Fig. 2) less than the trip point  $x_{tp}$ , and  $p_1 := 1 - p_2$ . Thus, the MAR is the sum of probabilities of all the no alarm states, i.e.,

$$\text{MAR} = P(\text{NA}_1) + P(\text{NA}_2) + \dots + P(\text{NA}_n).$$

The MAR is associated with  $p_1$ ,  $p_2$ , and  $n$  as given in the next proposition.

*Proposition 2:* For the  $n$ -sample alarm on/off delay, the MAR is

$$\text{MAR} = \frac{p_2^n(1+p_1+\dots+p_1^{n-1})}{p_2^n(1+p_1+\dots+p_1^{n-1}) + p_1^n(1+p_2+\dots+p_2^{n-1})}. \quad (13)$$

*Proof of Proposition 2:* For the Markov chain in Fig. 4, the matrix  $P \in \mathbb{R}^{2n \times 2n}$  of one step transition probability is

$$P = \begin{bmatrix} p_2 & p_1 & 0 & \dots & 0 & 0 & 0 & \dots & 0 \\ p_2 & 0 & p_1 & \dots & 0 & 0 & 0 & \dots & 0 \\ \vdots & \vdots & \vdots & \ddots & \vdots & \vdots & \vdots & \dots & \vdots \\ p_2 & 0 & \dots & 0 & p_1 & 0 & 0 & \dots & 0 \\ 0 & 0 & \dots & 0 & p_1 & p_2 & 0 & \dots & 0 \\ 0 & 0 & 0 & \dots & p_1 & 0 & p_2 & \dots & 0 \\ \vdots & \ddots & \vdots \\ 0 & 0 & 0 & \dots & p_1 & 0 & 0 & \dots & p_2 \\ p_2 & 0 & 0 & \dots & p_1 & 0 & 0 & \dots & 0 \end{bmatrix}.$$

Then, (13) can be proved by taking a procedure similar to that in the proof of Proposition 1.  $\square$

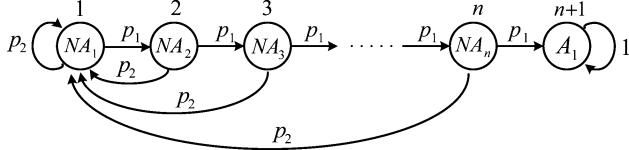


Fig. 5. Markov diagram of the  $n$ -sample on/off delay for the computation of AAD.

With respect to the AAD, the definition is the same as (3) in Section II, except that  $t_a$  refers to the time instant when the first alarm is raised by using the  $n$ -sample alarm on/off delay. It is reasonable to assume that the alarm is inactive at the time instant  $(t_0 - h)$  and do not consider the process of clearing the alarm once the alarm is raised. Hence, denote the state at the time instant  $(t_0 - h)$  as the first no-alarm state  $NA_1$  and the process is carried forward to the alarm state  $A_1$  with the same procedure in Fig. 4. Because here we are only concerned with the first alarm (when the state reaches to the alarm state  $A_1$  for the first time), only the top half of the Markov chain given in Fig. 4 is considered. In particular, when the state reaches to the alarm state  $A_1$ , it will stay in the state  $A_1$  with probability 1 for the computation of AAD. This operating mechanism is illustrated by the Markov chain in Fig. 5.

*Remark:* The state at the time instant  $(t_0 - h)$  does not have to be  $NA_1$ , and could be any one of the no-alarm states,  $NA_i$  for  $i = 1, \dots, n$ ; however, only the state  $NA_1$  is considered for two reasons. i) It is ready to obtain from the proof of Proposition 1 that the probability of being in the state  $NA_i$  is

$$P(NA_i) = \frac{q_1^{i-1} q_2^n}{q_1^n (1 + \dots + q_2^{n-1}) + q_2^n (1 + \dots + q_1^{n-1})}$$

where  $q_1$  is the probability of  $x$  in the normal condition with the PDF  $q(x)$  taking values greater than  $x_{tp}$ . Thus, the probability of starting with  $NA_1$  is much larger than the probability of the rest states combined, since  $q_1$  is usually quite small. ii) In practice, the normal and abnormal PDFs of  $x$  are usually not available and have to be estimated. If the state at the time instant  $(t_0 - h)$  is  $NA_i$  for  $i > 1$ , i.e., all the samples  $x(t_0 - ih), \dots, x(t_0 - h)$  are greater than  $x_{tp}$ , and  $x(t_0 - ih - h)$  is smaller than  $x_{tp}$ , then the proposed method for estimation of normal and abnormal PDFs in Section V would very likely classify  $x(t_0 - ih), \dots, x(t_0 - h)$  into the abnormal data section. Thus, the sample right before the detected change point from the normal to abnormal is less than  $x_{tp}$ , and the corresponding state is  $NA_1$ . Owing to these two reasons, we ignore the case that the time instant  $(t_0 - h)$  is associated with the other no-alarm state  $NA_i$  for  $i > 1$ .

*Proposition 3:* If the state at the time instant  $(t_0 - h)$  is  $NA_1$ , for the  $n$ -sample alarm on/off delay, the AAD is

$$\overline{T_d} = h \frac{(1 - p_1^n - p_2 p_1^n)}{p_2 p_1^n}. \quad (14)$$

*Proof of Proposition 3:* Define the states  $NA_1, NA_2, \dots, A_1$  as the states  $1, 2, \dots, n + 1$ , respectively.

According to the definition in (3), the AAD for the  $n$ -sample alarm on/off delay is

$$\overline{T_d} = E(T_d) = E(hT_{1,n+1}) - h \quad (15)$$

where  $T_{1,n+1}$  is the number of transmission steps taken from state 1 to the alarm state  $n + 1$ . The subtraction of  $h$  in (15) is owing to the fact that the state 1 occurs at the time instant  $(t_0 - h)$ .

The computation of  $E(T_{1,n+1})$  can be obtained as follows. First, the moment generating function of the discrete random variable  $T_{i,n+1}$ , for  $i \in \{1, 2, \dots, n + 1\}$  is

$$\Gamma_{i,n+1}(z) = \sum_{l=0}^{\infty} P_{i,n+1}^{(l)} z^l \quad (16)$$

where  $P_{i,n+1}^{(l)} := P(T_{i,n+1} = l)$  and  $z := e^t$  [15]. Differentiating  $\Gamma_{i,n+1}(z)$  with respect to  $z$  yields

$$\frac{d}{dz} \Gamma_{i,n+1}(z) = \sum_{l=0}^{\infty} l P_{i,n+1}^{(l)} z^{l-1}$$

which implies that the mean transmission step from state  $i$  to state  $n + 1$  is

$$E(T_{i,n+1}) = \sum_{l=0}^{\infty} l P_{i,n+1}^{(l)} = \left. \frac{d}{dz} \Gamma_{i,n+1}(z) \right|_{z=1}.$$

Thus,  $E(T_{1,n+1})$  in (15) can be calculated as

$$E(T_{1,n+1}) = \left. \frac{d}{dz} \Gamma_{1,n+1}(z) \right|_{z=1}. \quad (17)$$

Second, using the Chapman–Kolmogorov Equation ([15, pp. 705]), namely

$$P_{i,k}^{(l)} = \sum_{j \in I} P_{i,j}^{(1)} P_{j,k}^{(l-1)}$$

and the definitions in Markov chain theory

$$\begin{cases} P_{i,k}^{(0)} = 0, & \text{for } i \neq k \\ P_{i,k}^{(0)} = 1, & \text{for } i = k \end{cases}$$

(16) for  $i \neq n + 1$  becomes

$$\begin{aligned} \Gamma_{i,n+1}(z) &= \sum_{l=0}^{\infty} P_{i,n+1}^{(l)} z^l \\ &= P_{i,n+1}^{(0)} z^0 + \sum_{l=1}^{\infty} \sum_{j \in I} P_{i,j}^{(1)} P_{j,n+1}^{(l-1)} z^l \\ &= \left( \sum_{j \in I} z P_{i,j}^{(1)} \right) \left( \sum_{l=1}^{\infty} P_{j,n+1}^{(l-1)} z^{l-1} \right) \\ &= \sum_{j \in I} z P_{i,j}^{(1)} \Gamma_{j,n+1}(z) \end{aligned} \quad (18)$$

where  $I$  is the whole state-space  $\{1, 2, \dots, n+1\}$ . Since the state  $n+1$  is a recurrent state, (16) for  $i = n+1$  reduces to

$$\Gamma_{n+1,n+1}(z) = \sum_{l=0}^{\infty} P_{n+1,n+1}^{(l)} z^l = 1$$

which is obtained based on two definitions in Markov chain theory for a recurrent state  $k$

$$\begin{cases} P_{k,k}^{(l)} = 0, & \text{for } l > 0 \\ P_{k,k}^{(l)} = 1, & \text{for } l = 0 \end{cases}.$$

From (18) and the Markov chain in Fig. 5, we have

$$\begin{cases} \Gamma_{1,n+1}(z) = zp_2\Gamma_{1,n+1}(z) + zp_1\Gamma_{2,n+1}(z) \\ \Gamma_{2,n+1}(z) = zp_2\Gamma_{1,n+1}(z) + zp_1\Gamma_{3,n+1}(z) \\ \vdots \\ \Gamma_{n,n+1}(z) = zp_2\Gamma_{1,n+1}(z) + zp_1\Gamma_{n+1,n+1}(z) \end{cases}. \quad (19)$$

As  $\Gamma_{n+1,n+1}(z) = 1$ , solving (19) for  $\Gamma_{1,n+1}(z)$  gives

$$\Gamma_{1,n+1}(z) = \frac{zp_1^n}{1 - zp_2 - z^2p_2p_1 - \dots - z^n p_2 p_1^{n-1}}.$$

Therefore, (17) becomes

$$E(T_{1,n+1}) = \frac{d}{dz}\Gamma_{1,n+1}(z)\Big|_{z=1} = \frac{(1-p_1^n)}{p_2 p_1^n}$$

and the AAD in (15) is

$$\overline{T_d} = hE(T_{1,n+1}) - h = h \frac{(1-p_1^n - p_2 p_1^n)}{p_2 p_1^n}.$$

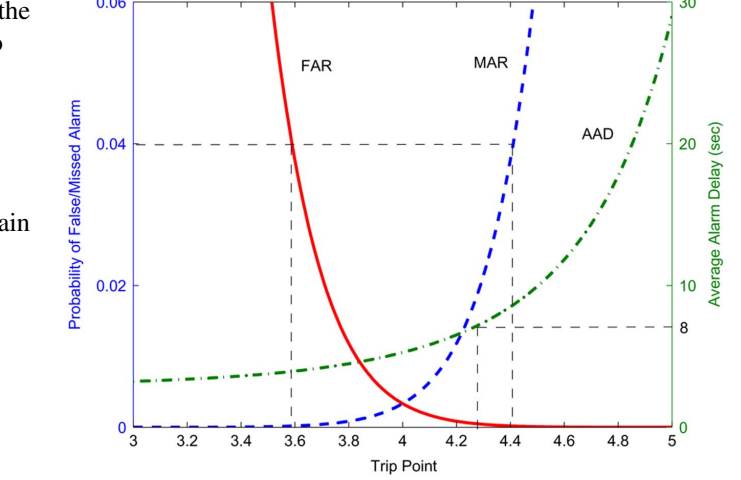


Fig. 6. The relation between FAR/MAR/AAD and the trip point.

the three performance indices. The design problem is formulated as

Given the PDFs of  $x(t)$  in the normal and abnormal conditions, how to choose the trip point and/or other design parameters of an alarm system to satisfy certain requirements on the FAR, MAR, and AAD?

Here, the alarm system could be the basic one in Section II, or the alarm on/off delay in Section III. For the later, the number of sample delay  $n$  is another design parameter along with the trip point  $x_{tp}$ . Because the basic alarm generating mechanism in Section II is the special case with  $n = 1$  for alarm on/off delay, the design procedure is presented here for the alarm on/off delay. Three cases will be investigated.

- Case I: Design  $x_{tp}$  for a fixed value of  $n$ .
- Case II: Design  $n$  for a fixed value of  $x_{tp}$ .
- Case III: Design both  $n$  and  $x_{tp}$ .

#### A. Case I: Design $x_{tp}$ for a Fixed Value of $n$

For a fixed value of  $n$ , the design of  $x_{tp}$  is based on two trade-offs between the FAR and MAR/AAD. Example 3 illustrates the design principle.

*Example 3:* The process variable  $x$  is generated in the same way as that in Example 1. The objective is to design  $x_{tp}$  for the alarm on/off delay with  $n = 4$  to meet the requirements:  $\text{FAR} \leq 4\%$ ,  $\text{MAR} \leq 4\%$ ,  $\text{AAD} \leq 8h$  for  $h = 1$  s.

Based on the PDFs in (5),  $q_1 = 0.1587$ ,  $q_2 = 1 - q_1$ ,  $p_2 = 0.1587$ ,  $p_1 = 1 - p_2$ . Then, from (6), (13) and (14), the relations between FAR/MAR/AAD and  $x_{tp}$  are obtained for the alarm on/off delay with  $n = 4$ , and are shown as the three plots in Fig. 6. Clearly, there are two tradeoffs between the FAR and MAR/AAD in Fig. 6. That is, when  $x_{tp}$  gets larger, FAR is decreasing but MAR and AAD are increasing, and *vice versa*. Hence, the requirements of FAR, MAR, and AAD will impose their own valid ranges of  $x_{tp}$  based on these tradeoffs. The intersection of these ranges will be the final choice of  $x_{tp}$  to meet all the requirements of FAR, MAR and AAD; if the intersection is empty, then there is no way to meet all the requirements by solely changing  $x_{tp}$ . For this example, based on the three plots in Fig. 6, satisfying the requirements on the FAR, MAR,

$$\text{FAR} = 0.0142, \text{ MAR} = 0.0142, \overline{T_d} = 3.2804.$$

In particular,  $q_1 = 0.1587$  (as computed in Example 1) is quite small so that (14) is expected to be accurate enough. To verify these theoretical values, the same types of Monte Carlo simulations as those in Example 1 are implemented to provide

$$\begin{aligned} m(\hat{\text{FAR}}) &= 0.0144, & s(\hat{\text{FAR}}) &= 0.0082 \\ m(\hat{\text{MAR}}) &= 0.0143, & s(\hat{\text{MAR}}) &= 0.0085 \\ m(\hat{\overline{T_d}}) &= 3.2805, & s(\hat{\overline{T_d}}) &= 0.0945, \end{aligned}$$

which are in line with the above theoretical values.  $\square$

#### IV. DESIGN OF ALARM SYSTEMS BASED ON THREE PERFORMANCE INDICES

With the above results for the FAR, MAR, and AAD, we are ready to design alarm systems in a systematic manner based on

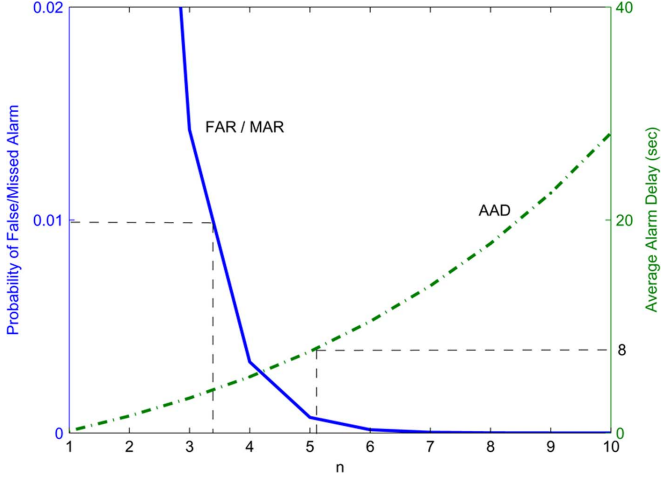


Fig. 7. The relation between FAR/MAR/AAD and the number of sample delay  $n$ .

and AAD demands the different ranges of  $x_{tp}$  as  $x_{tp} \geq 3.59$ ,  $x_{tp} \leq 4.41$ , and  $x_{tp} \leq 4.35$ , respectively. Their intersection provides the valid range  $x_{tp} \in [3.59, 4.35]$ .  $\square$

#### B. Case II: Design $n$ for a Fixed Value of $x_{tp}$

For the alarm on/off delay, the number of sample delay  $n$  is an extra design parameter. For a fixed value of  $x_{tp}$ , the design of  $n$  is based on two tradeoffs between the FAR/MAR and AAD. Example 4 illustrates the design principle.

*Example 4:* The process variable  $x$  is generated in the same way as that in Example 1. The objective is to choose  $n$  for the alarm on/off delay with a fixed value of  $x_{tp} = 4.0$  to meet the requirements:  $\text{FAR} \leq 1\%$ ,  $\text{MAR} \leq 1\%$ ,  $\text{AAD} \leq 8h$  for  $h = 1$  s.

Similar as in Example 3, the relations between FAR/MAR/AAD and  $n$  can be obtained from (6), (13), and (14) with the fixed value of  $x_{tp} = 4.0$ . The relations are shown as the three plots in Fig. 7, where exists two tradeoffs between the FAR/MAR and AAD. For a fixed value of  $x_{tp}$ , a larger value of  $n$  leads to decrements of FAR and MAR, but to an increment of AAD. These tradeoffs will confine the possible ranges of  $n$ , whose intersection is the final valid range of  $n$ . Based on the three plots in Fig. 7, it is straightforward to see that  $n = 4$  or  $n = 5$  is the choice to satisfy all the requirements.  $\square$

#### C. Case III: Design Both $n$ and $x_{tp}$

If both  $n$  and  $x_{tp}$  are free for design, the design procedure is more complex than those in Sections IV-A and IV-B. The basic principle is to determine the valid values of  $n$  first and design  $x_{tp}$  for each valid value of  $n$ . The design procedure is illustrated via the following example.

*Example 5:* The process variable  $x$  is generated in the same way as that in Example 1. The objective is to design  $x_{tp}$  and  $n$  for the alarm on/off delay to meet the requirements:  $\text{FAR} \leq 1\%$ ,  $\text{MAR} \leq 1\%$ ,  $\text{AAD} \leq 10h$  for  $h = 1$  s.

The design procedure goes as follows: First, based on (6) and (13), the plots of MAR versus FAR by varying  $x_{tp}$  for different values of  $n$  can be obtained in Fig. 8. The curves within the

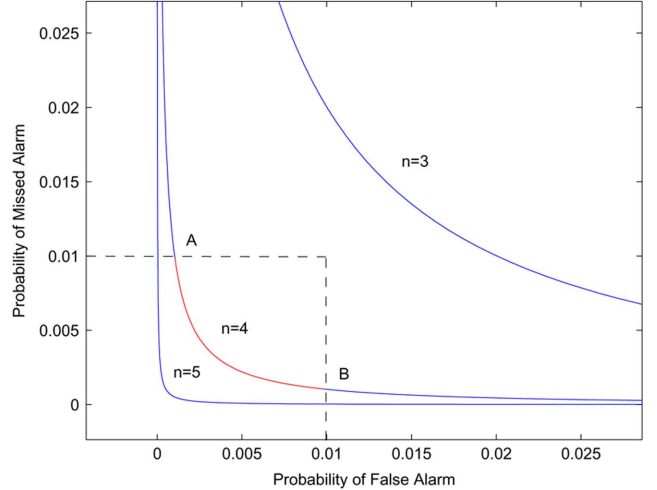


Fig. 8. The relation between FAR and MAR for alarm on/off delay.

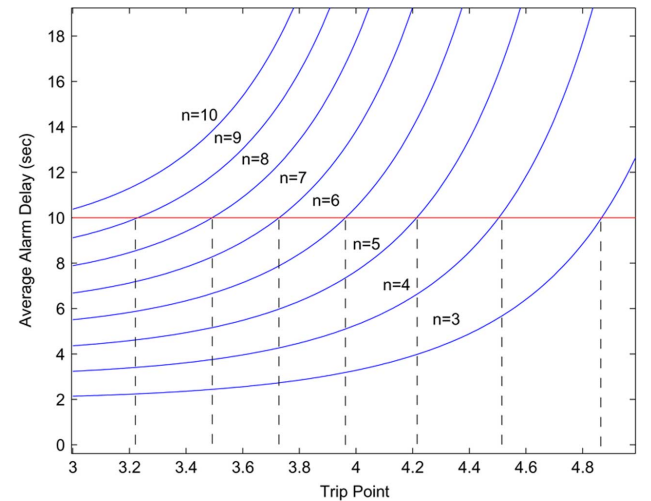


Fig. 9. The relation between AAD and trip point for alarm on/off delay.

small rectangle area in Fig. 8, e.g., the curve  $AB$  therein, can meet the requirements on FAR and MAR. These curves confine the valid range of  $n$  to be  $n \geq 4$ . Second, via (14), the relation between AAD and  $x_{tp}$  for difference values of  $n$  is plotted in Fig. 9, which says that the valid range of  $n$  is  $n \in [1, 9]$  in order to meet the requirement of AAD. Thus, the valid range of  $n$  is  $[4, 9]$ . For each value of  $n \in [4, 9]$ , the valid ranges of  $x_{tp}$  for satisfying the requirements of FAR and MAR are obtained from the corresponding curves shown in Fig. 8, and are listed in the second column of Table I; in order to satisfy the requirements of AAD, the valid ranges of  $x_{tp}$  are obtained from Fig. 9, and are the ones listed in the third column of Table I. Finally, we can select the intersection of the valid ranges in the second and third columns of Table I as the proper range of  $x_{tp}$  for each value of  $n$ .  $\square$

Table I provides the valid ranges of  $n$  and  $x_{tp}$ . However, only one pair of values of  $n$  and  $x_{tp}$  can be implemented in the alarm system. Thus, it is necessary to choose the optimal values of  $n$  and  $x_{tp}$  in some manner. Depending on the preference on FAR, MAR, and AAD for each specific situation in practice, different optimization criteria can be formulated to obtain the

TABLE I  
THE VALID RANGES OF  $x_{tp}$  FOR EACH VALUE OF  $n \in [4, 9]$

$n$	$x_{tp}(\text{FAR}, \text{MAR})$	$x_{tp}(\text{AAD})$	$x_{tp}$
4	[3.83, 4.17]	[3.4, 5.0]	[3.83, 4.17]
5	[3.67, 4.33]	[3.4, 2.1]	[3.67, 4.21]
6	[3.56, 4.44]	[3.3, 9.6]	[3.56, 3.96]
7	[3.47, 4.53]	[3.3, 7.2]	[3.47, 3.72]
8	[3.41, 4.59]	[3.3, 4.9]	[3.41, 3.49]
9	[3.36, 4.64]	[3.3, 2.2]	$\emptyset$

TABLE II  
THE OPTIMAL VALUE OF  $x_{tp}$  AND THE MINIMAL LOSS FUNCTION  $J(x_{tp}, n)$  FOR EACH VALID VALUE OF  $n$

$n$	$x_{tp}$	minimal value of $J(x_{tp}, n)$
4	3.97	1.7063
5	3.88	1.5762
6	3.76	1.7764
7	3.65	2.0171
8	3.49	2.3708

optimal values of  $n$  and  $x_{tp}$ . One possible choice is to minimize AAD subject to some upper bounds of FAR and MAR. Despite the variation of optimization criterion, the optimal values of  $n$  and  $x_{tp}$  have to be obtained by following the same principle. Hence, we may choose a weighted-sum loss function as

$$J(x_{tp}, n) = \omega_1 \frac{\text{FAR}}{\text{RFAR}} + \omega_2 \frac{\text{MAR}}{\text{RMAR}} + \omega_3 \frac{\text{AAD}}{\text{RAAD}} \quad (20)$$

to illustrate the principle. Here, RFAR, RMAR, and RAAD are the requirements of FAR, MAR, and AAD, respectively, and  $\omega_1$ ,  $\omega_2$ , and  $\omega_3$  are the weights of FAR, MAR, and AAD, respectively. Then, the optimal values of  $x_{tp}$  and  $n$  are the ones minimizing the loss function in (20), i.e.,

$$(x_{tp}, n) = \arg \min J(x_{tp}, n).$$

Since the FAR, MAR, and AAD, respectively, given in (6), (13), and (14) are nonlinear functions of  $n$  and  $x_{tp}$ , a two-dimensional grid search is implemented to find the optimal values of  $x_{tp}$  and  $n$ .

*Example 6:* Let us continue the design procedure in Example 5, where RFAR = 1%, RMAR = 0.01, and RAAD = 10h. Suppose that these three performance indices are equally important so that  $\omega_1 = 1$ ,  $\omega_2 = 1$ , and  $\omega_3 = 1$ . The two-dimensional grid search method is exploited to search for the optimal values of  $x_{tp}$  and  $n$ , within their valid ranges given in Table I from Example 5. For each valid values of  $n$ , the corresponding optimal value of  $x_{tp}$  and the minimal loss function  $J(x_{tp}, n)$  are listed in Table II, which gives the optimal values  $n = 5$  and  $x_{tp} = 3.88$ . Here, the step size in the grid search of  $x_{tp}$  is chosen to be 0.01.  $\square$

## V. ESTIMATION OF PDFS

This section proposes a new method to estimate the PDFs of the process variable  $x$  in the normal and abnormal conditions,

which are required for the calculation of the FAR, MAR, and AAD. To be specific, the PDFs estimation problem is described as:

Given the collected data  $\{x(t)\}_{t=1}^T$  of the process variable  $x$ , how to estimate the PDFs of  $x(t)$  in the normal and abnormal conditions?

The critical step to solve this problem is to separate the normal and abnormal sections of  $\{x(t)\}_{t=1}^T$ . Doing so is possible under the following assumptions.

- A1) The two PDFs of  $x$  in the normal and abnormal conditions have different mean values;
- A2) The process knowledge that the mean values belong to either the normal condition or the abnormal one is known *a priori*.

Assumption A1 says that the process variable  $x$  experiences some mean changes; hence, we exploit the mean change detection techniques to locate the mean change points in  $\{x(t)\}_{t=1}^T$ . For Assumption A2, the current value of  $x_{tp}$  usually is a good threshold for the mean values to be compared with. For instance, if  $x_{tp}$  stands for a high-value alarm trip point, then a data section having the mean value statistically larger than  $x_{tp}$  will belong to the abnormal condition.

There are a wide range of change detection techniques in literature, e.g., Shewhart chart, moving average charts, cumulative sum procedures, generalized likelihood ratio test, Bayesian and information criterion approaches [3], [6]. Most of these techniques are parametric in assuming the initial distribution or the signal model structure to be known *a priori*, e.g.,  $x$  is a Gaussian random process or takes the autoregressive model structure. However, usually it is very difficult to know this kind of information in practice. In addition, the collected data  $\{x(t)\}_{t=1}^T$  may contain multiple mean changes instead of a single one.

The proposed method of estimating the PDFs is based on the nonparametric approach for one mean-change point detection proposed by Pettitt [16]. This non-parametric approach does not suffer from the above-mentioned problems for parametric change detection techniques, and is very effective in detecting change of mean values. However, it cannot be used directly to find multiple change points. Here we revise it by adopting the idea of bisection method. The proposed method is an offline method to estimate the normal and abnormal PDFs for historical data  $\{x(t)\}_{t=1}^T$ ; it consists of the following steps:

Step 1: For  $\{x(t)\}_{t=1}^T$ , find one mean change point as follows [16]:

- Calculate the test statistic  $U_{1,T} = V_{1,T}$  and  $U_{t,T} = U_{t-1,T} + V_{t,T}$  for  $t = 2, 3, \dots, T$ , where

$$V_{t,T} = \sum_{j=1}^T \text{sgn}(x(t) - x(j)).$$

- Find the time instant  $t_{\max}$  maximizing  $|U_{t,T}|$  and compute the corresponding P-value as

$$P = 2 \exp \left( \frac{-6 \max_{1 \leq t < T} |U_{t,T}|^2}{T^2 + T^3} \right).$$

- Choose the probability of type I error  $\alpha$ , e.g.,  $\alpha = 0.01$ , and define the null hypothesis, namely,  $x(t_{\max})$  is not a mean change point. If  $P < \alpha$ , reject the null hypothesis so that  $x(t_{\max})$  is the change point of  $\{x(t)\}_{t=1}^T$ . If  $P > \alpha$ , the null hypothesis cannot be rejected and no change point can be found.

Step 2: Divide  $\{x(t)\}_{t=1}^T$  into two subsections:  $\{x_1(t)\}_{t=1}^{t_{\max}}$  and  $\{x_2(t)\}_{t=t_{\max}+1}^T$  according to  $t_{\max}$ . Go to Step 1 for each subsection to find their own one change point. Repeat Steps 1 and 2 until no further change points can be found.

Step 3: After finding all the change points,  $\{x(t)\}_{t=1}^T$  has been isolated into several data sections. For each data section, the sample mean is calculated and compared with the trip point  $x_{tp}$ . Here, a standard T-test (see, e.g., [20, Section 10.7]) is used for the comparison as follows. Let one of the data sections be denoted as  $\{x(t)\}_{t=t_0}^{t_1}$ . For this data section, the Student's  $t$ -distributed statistic is computed

$$t = \frac{\bar{x} - x_{tp}}{s/\sqrt{t_1 - t_0}}.$$

Here,  $\bar{x}$  and  $s$  are the sample mean and standard deviation of  $x$ , respectively, i.e.,

$$\begin{aligned} \bar{x} &= \frac{\sum_{t=t_0}^{t_1} x(t)}{t_1 - t_0 + 1} \\ \text{and} \\ s &= \sqrt{\frac{\sum_{t=t_0}^{t_1} (x(t) - \bar{x})^2}{t_1 - t_0}}. \end{aligned}$$

If  $t$  is larger (smaller) than the critical value  $t_{\beta, t_1 - t_0}$  ( $-t_{\beta, t_1 - t_0}$ ), then the sample mean  $\bar{x}$  is statistically larger (smaller) than  $x_{tp}$ , and this data section is regarded as the one in the abnormal (normal) condition; otherwise,  $\bar{x}$  is statistically equal to  $x_{tp}$ , and this data section is discarded and not included in the subsequent PDF estimation. Here, the probability of type I error is denoted as  $\beta$ , e.g.,  $\beta = 0.05$ . All the data sections regarded in the abnormal (normal) conditions are put together into one single group, referred to as the abnormal (normal) data.

Step 4: The PDFs of  $x$  in the normal and abnormal conditions are now ready to be estimated based on the normal and abnormal data obtained in Step 3. Here, the kernel-based method is used to estimate the PDFs, using the Gaussian kernel function (see, e.g., [18])

$$K(x) = \frac{1}{\sqrt{2\pi}} \exp(-x^2/2).$$

*Example 7:* This example illustrates the proposed method for the estimation of the PDFs. The collected data of  $x$  is generated as

$$\begin{cases} x(t) \sim N(0, 0.5^2), & t < 500 \\ x(t) \sim \Gamma(3, 0.7), & 500 \leq t < 1300 \\ x(t) \sim N(0, 0.5^2), & 1300 \leq t < 1800 \\ x(t) \sim \Gamma(3, 0.7), & 1800 \leq t < 2600 \\ x(t) \sim N(0, 0.5^2), & 2600 \leq t \leq 3100 \end{cases}.$$

Thus,  $x$  experiences mean changes at the time instants 500, 1300, 1800, 2600, with Gaussian and Gamma PDFs as the

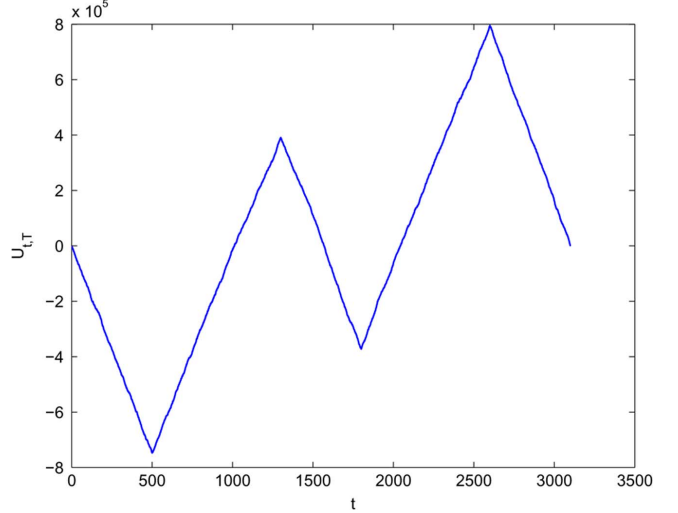


Fig. 10.  $U_{t,T}$  for the data section  $x(1 : 3100)$ .

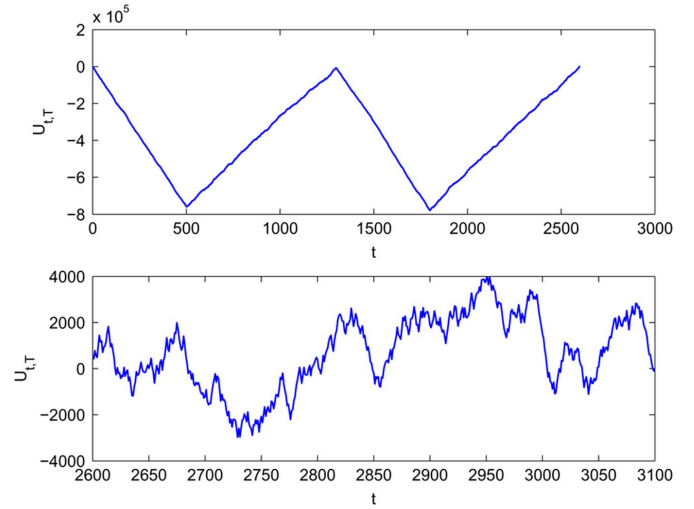


Fig. 11.  $U_{t,T}$  for the data subsections  $x(1 : 2599)$  (top) and  $x(2600 : 3100)$  (bottom).

normal and abnormal distributions, respectively. The trip point is  $x_{tp} = 1$ .

First, for the whole collected data  $x(1 : 3100)$ , the test statistic  $U_{t,T}$  is calculated, as shown in Fig. 10. The time instant maximizing  $|U_{t,T}|$  is  $t = 2600$  with the P-value  $P = 1.03 \times 10^{-55}$ . Choose the probability of type I error to be  $\alpha = 0.01$ . As  $P < \alpha$ , the time instant 2600 is correctly detected as a mean change point.

Second, for the data sections  $x(1 : 2599)$  and  $x(2600 : 3100)$ , the test statistics  $U_{t,T}$  are shown in Fig. 11. The maxima of  $|U_{t,T}|$  are located at  $t = 502$  with  $P = 1.25 \times 10^{-172}$  and  $t = 2954$  with  $P = 0.9457$ , respectively. The former P-value is less than  $\alpha$ , while the latter one is not. Thus, we reach two correct conclusions: the time instant 502 is a mean change point for the data section  $x(1 : 2599)$ , while the data section  $x(2600 : 3100)$  has no mean change.

Similarly, the procedure is repeated until no further change points can be found. Here, the procedure stops at the fourth iteration. The detected change points and the corresponding P-values are listed in Table III.

TABLE III  
THE DETECTED CHANGE POINTS AND THE CORRESPONDING P-VALUES

Change Points	P-value
502	$1.25 \times 10^{-172}$
1300	$1.47 \times 10^{-67}$
1800	$9.31 \times 10^{-91}$
2600	$1.03 \times 10^{-55}$

TABLE IV  
CLASSIFICATION OF ISOLATED DATA SECTIONS INTO THE NORMAL AND ABNORMAL DATA

Normal Data	Abnormal Data
$x(1:501)$	$x(502:1299)$
$x(1300:1799)$	$x(1800:2599)$
$x(2600:3100)$	

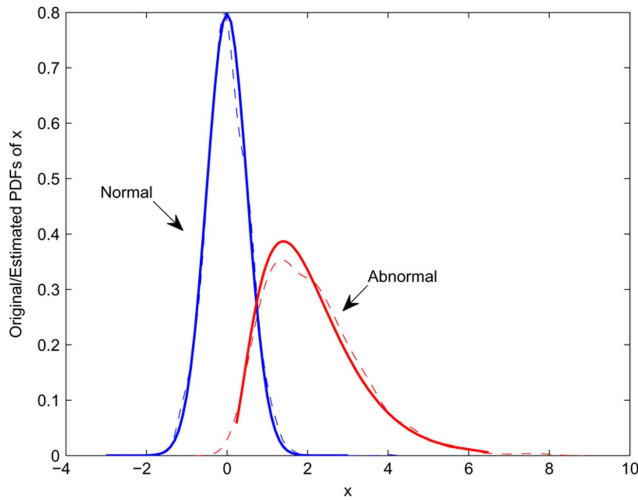


Fig. 12. The estimated PDFs based on the normal and abnormal data (solid line: original PDFs; dashed line: estimated PDFs).

Next, as described in Step 3, the normal and abnormal data are obtained based on all the detected change points and  $x_{tp} = 1$ . The classification of the isolated data sections are given in Table IV, using the probability of type I error  $\beta = 0.01$ . Finally, the two PDFs for  $x$  in the normal and abnormal conditions are estimated via the kernel-based method, as shown in Fig. 12, where the true PDFs are given as well for the purpose of comparison.

## VI. INDUSTRIAL CASE STUDY

In this section, an industrial case study is presented to illustrate the procedure of assessing the performance of an alarm system, and redesigning the corresponding parameters of the alarm system to meet with the requirements of FAR, MAR, and AAD.

The process variable  $x$  is the pressure of the main steam driving the power turbine for a thermal power plant at Weifang, Shandong Province, China. Owing to the time-varying operating conditions, the steam pressure experiences a large scale of amplitude variations. The current alarm system for the steam pressure is the basic one in Section II, with the trip point  $x_{tp} = 23.6$ . When the amplitude is less than 23.6, an alarm will be

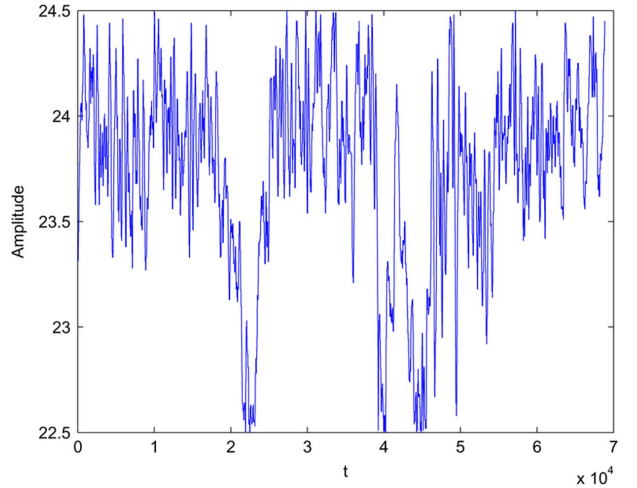


Fig. 13. The time trend of the industrial process variable.

TABLE V  
THE DETECTED CHANGE POINTS AND THE CORRESPONDING P-VALUES

Change Point	P-value
9395	$1.10 \times 10^{-144}$
18354	0
25065	0
33886	$6.80 \times 10^{-72}$
39063	0
46135	0
54410	0
63505	$9.59 \times 10^{-228}$

raised. From the DCS database,  $6.8 \times 10^4$  data points, shown in Fig. 13, are collected with the sampling period  $h = 1$  s, standing for the routine operation of the thermal power plant for 19 h on July 3, 2010.

Our objective is to assess the current performance of the alarm systems and to design the parameters of the alarm system if necessary, in order to satisfy the requirements:  $\text{FAR} \leq 5\%$ ,  $\text{MAR} \leq 5\%$ ,  $\text{AAD} \leq 5$  s.

The very first step is to estimate the PDFs of  $x$  in the normal and abnormal conditions via the proposed method in Section V. The detected change points and the corresponding P-values are listed in Table V; here the probability of type I error is chosen to be  $\alpha = 0.05$ . By comparing with the trip point  $x_{tp} = 23.6$ , using the hypothesis tests (the probability of type I error is  $\beta = 0.05$ ) in Step 3 of Section V, the isolated data sections are classified into the groups of normal and abnormal data, as given in Table VI. The estimated PDFs based on the normal and abnormal data are shown in Fig. 14.

Second, using the estimated PDFs in Fig. 14, the current performance indices of the alarm system are respectively obtained by (1), (2), and (4),  $\text{FAR} = 14.86\%$ ,  $\text{MAR} = 12.04\%$ , and  $\text{AAD} = 0.1369$  s. The FAR and MAR are much larger than their requirements, and the alarm system needs to be redesigned.

We consider designing  $x_{tp}$  with the basic alarm generation mechanism unchanged. This is a special case for the number of sample delay  $n = 1$  in Case I at Section IV-A. According to the relation between FAR/MAR/AAD and  $x_{tp}$ , the requirements of  $\text{FAR} \leq 5\%$  and  $\text{MAR} \leq 5\%$  impose the valid ranges of  $x_{tp}$

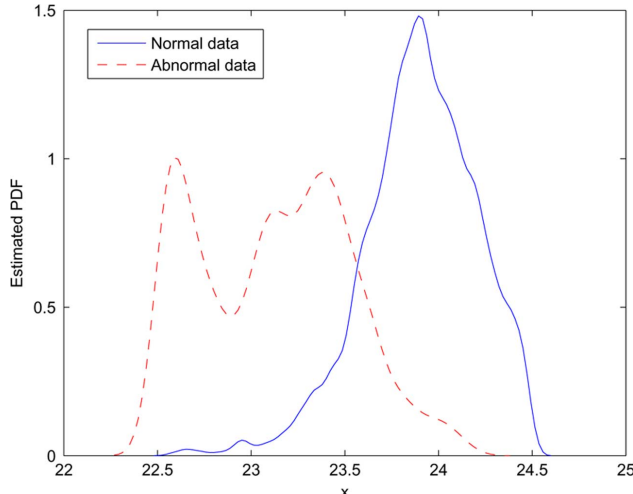


Fig. 14. The estimated PDFs for normal and abnormal data.

TABLE VI  
CLASSIFICATION OF ISOLATED DATA SECTIONS INTO THE  
NORMAL AND ABNORMAL DATA

Normal Data	Abnormal Data
x(1:18353)	x(18354:25064)
x(25065:39062)	x(39063:46134)
x(46135:68873)	

TABLE VII  
PERFORMANCE INDICES AFTER DESIGNING  $n$  FOR THE  
FIXED VALUE OF  $x_{tp} = 23.6$

n	FAR	MAR	AAD
2	0.0468	0.0305	1.4294
3	0.0116	0.0060	2.8988
4	0.0025	0.0010	4.5694

TABLE VIII  
THE VALID RANGES OF THE TRIP POINT  $x_{tp}$  FOR  
DIFFERENT VALUES OF  $n$

n	$x_{tp}$ (FAR,MAR)	$x_{tp}$ (AAD)	$x_{tp}$
2	[23.55,23.60]	[23.15,24]	[23.55,23.60]
3	[23.45,23.70]	[23.40,24]	[23.45,23.70]
4	[23.38,23.76]	[23.58,24]	[23.58,23.76]
5	[23.34,23.78]	[23.77,24]	[23.77,23.78]

to be  $x_{tp} \in [23, 23.37]$  and  $x_{tp} \in [23.79, 24]$ , respectively. The two ranges have no intersection; as a result, it is impossible to satisfy all the three requirements by simply designing  $x_{tp}$ .

Next, we use the alarm on/off delay and design the number of sample delay  $n$  for the current trip point  $x_{tp} = 23.6$ . Following the design procedure in Section IV-B, the three requirements FAR, MAR, and AAD confine the valid ranges of  $n$  to be  $n > 1$ ,  $n > 1$ , and  $n < 5$  respectively, based on the relation between FAR/MAR/AAD and  $n$ . Hence, the valid range of  $n$  to meet with all the three requirements is  $1 < n < 5$ , and the performance indices after design are listed in Table VII.

We can follow the procedure in Section IV-C to design  $x_{tp}$  and  $n$ , if both parameters are free to be changed. According to the relation between FAR and MAR and the relation between AAD and  $x_{tp}$ , the valid ranges of  $x_{tp}$  and  $n$  are given

TABLE IX  
MINIMAL VALUES OF THE LOSS FUNCTION FOR  
DIFFERENT VALUES OF  $n$  AND  $x_{tp}$

n	$x_{tp}$	minimal value of loss function
2	23.58	7.7036
3	23.58	2.2133
4	23.59	1.2548
5	23.77	3.8856

in Table VIII. If necessary, we can also take the same path in Example 6 to search for the optimal values of  $n$  and  $x_{tp}$ . Here, the weights in (20) are chosen as  $\omega_1 = \omega_2 = \omega_3 = 1$ . The two-dimensional grid search is implemented to find out the optimal values within the valid ranges given in Table VIII. The minimal values of the loss function for different values of  $n$  and  $x_{tp}$  are listed in Table IX, which says that the optimal parameters are  $n = 4$  and  $x_{tp} = 23.59$ .

## VII. CONCLUSION

This paper studied the performance assessment and systematic design for univariate alarm systems, based on three performances indices, namely, FAR, MAR, and AAD. Equations (1), (2), and (4) gave the FAR, MAR, and AAD for the basic mechanism of alarm generation solely based on a trip point, while (6), (13), and (14) presented the counterparts for alarm on/off delay. The computation of FAR, MAR, and AAD was validated via simulation in Examples 1 and 2. Three cases were investigated for the systematic design of the trip point and/or the number of sample delay, based on the three performance indices. A new method was proposed to estimate the PDFs of the process variable in the normal and abnormal conditions. Numerical examples and an industrial case study were provided to illustrate the design procedure, the effectiveness of the proposed method in estimating two PDFs, and the application of the performance assessment and design of alarm systems in practice.

In this paper, the FAR, MAR, and AAD are developed under the assumption that the process variable  $x$  is IID, which is certainly not satisfied in some practical situations. For instance, the change from the normal to abnormal condition may experience some dynamic variation instead of an abrupt change. As a result, the derived expressions, e.g., (6), (13), and (14), may yield biased estimates. Thus, one of the future studies is to devise ways to compute FAR, MAR, and AAD for these more complicated situations. In addition, there are some other alarm generation mechanisms frequently adopted in industry, along with the basic one and alarm on/off delay in this paper. Another future work is to study the performance assessment and design problems for these alarm systems.

## ACKNOWLEDGMENT

The authors would like to thank the Associate Editor and anonymous reviewers for their constructive comments and helpful suggestions.

## REFERENCES

- [1] J. Ahnlund, T. Bergquist, and L. Spaanenburg, "Rule-based reduction of alarm signals in industrial control," *J. Intell. Fuzzy Syst.*, vol. 14, pp. 73–84, 2003.

- [2] *Management of Alarm Systems for the Process Industries*, ANSI/ISA-18.2, Jun. 2009.
- [3] M. Basseville and I. V. Nikiforov, *Detection of Abrupt Changes: Theory and Application*. Englewood Cliffs, NJ: Prentice-Hall, 1993.
- [4] M. L. Bransby and J. Jenkinson, *The Management of Alarm Systems*. New York: Health and Safety Executive, 1998.
- [5] R. Brooks, R. Thorpe, and J. Wilson, "A new method for defining and managing process alarms and for correcting process operation when an alarm occurs," *J. Hazardous Materials*, vol. 115, pp. 169–174, 2004.
- [6] J. Chen and A. K. Gupta, *Parametric Statistical Change Point Analysis*. Boston, MA: Birkhauser, 2000.
- [7] Y. Cheng, I. Izadi, and T. Chen, "On optimal alarm filter design," in *Proc. Int. Symp. Advanced Control of Ind. Process.*, Hangzhou, China, 2011, pp. 139–145.
- [8] A. Henningsen and J. P. Kemmerer, "Intelligent alarm handling in cement plants," *IEEE Ind. Appl. Mag.*, pp. 9–15, Sep./Oct. 1995.
- [9] M. Hollender and C. Beuthel, "Intelligent alarming," *ABB Review*, vol. 1, pp. 20–23, 2007.
- [10] A. J. Hugo, "Estimation of Alarm Settings," U.S. Patent US6 6618691B, Sep. 9, 2003.
- [11] A. J. Hugo, "Estimation of alarm deadbands," in *Proc. 7th IFAC Symp. Fault Detection, Supervision and Safety of Tech. Process.*, Barcelona, Spain, 2009, pp. 663–667.
- [12] I. Izadi, S. L. Shah, D. Shook, S. R. Kondaveeti, and T. Chen, "Optimal alarm design," in *Proc. 7th IFAC Symp. Fault Detection, Supervision and Safety of Tech. Process.*, Barcelona, Spain, 2009, pp. 651–656.
- [13] I. Izadi, S. L. Shah, D. Shook, and T. Chen, "An introduction to alarm analysis and design," in *Proc. 7th IFAC Symp. Fault Detection, Supervision and Safety of Tech. Process.*, Barcelona, Spain, 2009, pp. 645–650.
- [14] J. Liu, K. W. Lim, W. K. Ho, K. C. Tan, R. Srinivasan, and A. Tay, "The intelligent alarm management system," *IEEE Software*, pp. 66–71, 2003.
- [15] A. Papoulis and S. U. Pillai, *Probability, Random Variables and Stochastic Processes*, 4th ed. New York: McGraw-Hill, 2002.
- [16] A. N. Pettitt, "A non-parametric approach to the change-point problem," *Appl. Stat.*, vol. 28, pp. 126–135, 1979.
- [17] D. Rothenberg, *Alarm Management for Process Control*. Highland Park, NJ: Momentum Press, 2009.
- [18] B. W. Silverman, *Density Estimation for Statistics and Data Analysis*. London, U.K.: Chapman & Hall, 1986.
- [19] R. Srinivasan, J. Liu, K. W. Lim, K. C. Tan, and W. K. Ho, "Intelligent alarm management in a petroleum refinery," *Hydrocarbon Process.*, vol. 83, pp. 47–53, 2004.
- [20] R. E. Walpole, R. H. Myers, S. L. Myers, and K. Ye, *Probability and Statistics for Engineers and Scientists*, 8th ed. Englewood Cliffs: Prentice-Hall, 2006.
- [21] J. Xu and J. Wang, "Averaged alarm delay and systematic design for alarm systems," in *Proc. 49th IEEE Conf. Decision and Control*, Atlanta, GA, Dec. 15–17, 2010, pp. 6821–6826.
- [22] F. Yamanaka and T. Nishiya, "Application of the intelligent alarm system for the plant operation," *Computer Chem. Eng.*, vol. 21, pp. s625–s630, 1997.
- [23] F. Yang, S. L. Shah, and D. Xiao, "Correlation analysis of alarm data and alarm limit design for industrial processes," in *Proc. 2010 Amer. Control Conf.*, Baltimore, MD, 2010, pp. 5850–5855.
- [24] Y. Yuki, "Alarm system optimization for increasing operations productivity," *ISA Trans.*, vol. 41, pp. 383–387, 2002.



**Jianwei Xu** received the B.E. degree in automatic control from Jiangsu University, Jiangsu, China, in 2007. Currently, he is working towards the M.E. degree in the Department of Industrial Engineering and Management, College of Engineering, Peking University, China.

His current research topic is the advanced alarm system management.



**Jiandong Wang** received the B.E. degree in automatic control from Beijing University of Chemical Technology, Beijing, China, in 1997, and the M.Sc. and Ph.D. degrees from the University of Alberta, Edmonton, AB, Canada, in 2003 and 2007, respectively, all in electrical and computer engineering.

From 1997 to 2001, he was a Control Engineer with the Beijing Tsinghua Energy Simulation Company, Beijing. From February 2006 to August 2006, he was a Visiting Scholar at the Department of System Design Engineering, Keio University, Japan. Since December 2006 to present, he has been an Associate Professor with the Department of Industrial Engineering and Management, College of Engineering, Peking University, China. His current research interests include system identification, alarm systems, process monitoring and management, and their applications to industrial problems.

Dr. Wang received the ExxonMobil Fellowship in 2010 and P&G Fellowship in 2008 from Peking University.



**Iman Izadi** received the B.Sc. degree from Sharif University of Technology, Tehran, Iran, in 1997, the M.Sc. degree from the Isfahan University of Technology, Isfahan, Iran, in 2000, and the Ph.D. degree from the University of Alberta, Edmonton, Canada, in 2006, all in electrical engineering.

After graduation, he joined Matrikon (now part of Honeywell Process Solutions) as a Research Engineer. He is presently an Alarm Management Engineer at Honeywell Process Solutions. He is also the Research Manager of the Advances in Alarm Management and Design Group, a joint research group between the Departments of Electrical and Computer Engineering and Chemicals and Materials Engineering at the University of Alberta. He has developed a number of software tools for alarm management and rationalization. He has also implemented alarm management solutions in industrial plants in North America.



**Tongwen Chen** (F'06) received the B.Eng. degree in automation and instrumentation from Tsinghua University, Beijing, China, in 1984, and the M.A.Sc. and Ph.D. degrees in electrical engineering from the University of Toronto, Toronto, ON, Canada, in 1988 and 1991, respectively.

He is presently a Professor of Electrical and Computer Engineering at the University of Alberta, Edmonton, Canada. His research interests include computer and network based control systems, and their applications to the process and power industries.

Dr. Chen is a Fellow of the Engineering Institute of Canada. He is a registered Professional Engineer in Alberta, Canada. He has served as an Associate Editor for several international journals, including the *IEEE TRANSACTIONS ON AUTOMATIC CONTROL*, *Automatica*, and *Systems and Control Letters*.